

Impact of Polycyclic Aromatic Hydrocarbons on Barrier Function Toxicity in 3D Lung Model
from Normal and Asthmatic Donor Cells

by
Celine Huynh

A THESIS

submitted to

Oregon State University

Honors College

in partial fulfillment of
the requirements for the
degree of

Honors Baccalaureate of Science in BioResource Research
(Honors Scholar)

Presented May 29, 2020
Commencement June 2020

AN ABSTRACT OF THE THESIS OF

Celine Huynh for the degree of Honors Baccalaureate of Science in BioResource Research presented on May 29, 2020. Title: Impact of Polycyclic Aromatic Hydrocarbons on Barrier Function Toxicity in 3D Lung Model from Normal and Asthmatic Donor Cells.

Abstract approved: _____

Susan C. Tilton

Polycyclic aromatic hydrocarbons (PAHs) are known to cause adverse health effects in the human lung. Here, we evaluated biomarkers relevant for PAH toxicity in a 3D human primary bronchial epithelial cell (HBEC) model collected from normal and asthmatic donors. We previously found that PAHs decrease cellular barrier function integrity, which can lead to increased permeability, inflammation, and oxidative stress of the airway epithelium and contribute to the pathogenesis of lung disease. Therefore, we hypothesized that normal and diseased cells may have different sensitivity to PAH exposure in inflammation and cell junction-related biomarkers. Primary HBEC were exposed to benzo[a]pyrene (BaP), dibenzo[def,p]chrysene (DBC), and coal tar (CTE). A ROS detection assay found differences in sensitivity for BaP and CTE-exposed cells and no differences for DBC-exposed cells. RNAseq from normal cells treated with concentrations of BaP was used to identify dose-responsive pathways and biomarkers for future comparison with diseased cells. Development and cell adhesion pathways were modelled as a dose-response across BaP exposure using vector quantization and hierarchical clustering. Benchmark dose modelling identified regulation of cytoskeleton rearrangement as the most sensitive pathway. These results suggest that individuals with preexisting conditions may be at greater risk of developing COPD when exposed to air pollutants.

Key Words: Toxicity, Barrier Function, Sensitivity

Corresponding e-mail address: huynhce@oregonstate.edu

©Copyright by Celine Huynh
May 29, 2020

Impact of Polycyclic Aromatic Hydrocarbons on Barrier Function Toxicity in 3D Lung Model
from Normal and Asthmatic Donor Cells

by
Celine Huynh

A THESIS

Submitted to
Oregon State University
Honors College

In partial fulfillment of
the requirements for the
degree of

Honors Baccalaureate of Science in BioResource Research
(Honors Scholar)

Presented May 29, 2020
Commencement June 2020

Honors Baccalaureate of Science in BioResource Research project of Celine Huynh presented on May 29, 2020

APPROVED:

Susan C. Tilton, Mentor, representing Environmental and Molecular Toxicology

Katharine G. Field, Committee member, representing BioResource Research

Yvonne Chang, Committee member, representing Environmental and Molecular Toxicology

Toni Doolen, Dean, Oregon State University Honors College

I understand that my project will become part of the permanent collection of Oregon State University, Honors College. My signature below authorizes release of my project to any reader upon request.

Celine Huynh, Author

Introduction (864/750)

Polycyclic aromatic hydrocarbons

Polycyclic aromatic hydrocarbons (PAH)s are a class of environmental pollutants that contain at least two bonded aromatic rings (Siddens et al., 2015). They are both naturally occurring and emitted through fossil fuel combustion, vehicle exhaust, cigarette smoke, and other sources of incomplete combustion. PAH exposure occurs through inhalation, ingestion and skin contact. Exposure is not to individual PAHs; they often occur in mixtures. Some PAHs are known to have carcinogenic and mutagenic effects in humans while others are relatively benign. The degree of toxicity depends on the mixture and structure of the compound (Siddens et al., 2012). PAH exposure is associated with adverse health effects in the human lung, including cancer and elevated inflammation (Shi, Godschalk, and van Schooten, 2017). PAHs have varying abilities to induce reactive oxygen species (ROS); in the body, ROS can damage DNA, proteins, and lipids, triggering inflammatory responses (Yang et al. 2016). The Environmental Protection Agency's current approach to risk assessment for PAHs is to use Benzo[a]pyrene (BaP) as a reference PAH. BaP is classified as a known carcinogen by the International Agency for the Research on Cancer (IARC, 2010). However, the differences in sensitivity to PAH exposure between normal and diseased cells is poorly understood. This study focuses on three PAHs: Benzo[a]pyrene (BaP), Dibenzo[def,p]chrysene (DBC), and Coal Tar Extract (CTE), and the impact of these PAHs on inflammation and cell junction-related biomarkers.

3D Human Bronchial Epithelial Cell Model

Primary human bronchial epithelial cells (HBEC) were employed to evaluate PAH toxicity and the impact of donor diseased state. HBEC can be collected from bronchial brushings

of donors and are cultured at the air-liquid interface (ALI). These cells are then differentiated into a three-dimensional-structure with multiple cell types similar to the bronchial epithelium *in vivo*. These cells include ciliated cells, mucus-producing goblet cells, and mitotically active basal cells. Cells that are grown in 3D are believed to be more predictive to toxicity compared to cells grown in monolayer culture due to their multidimensional structure and enhanced metabolic activity (Kimlin, 2013). Cells that are grown in a 2D culture fail to represent the complex architecture of the extracellular matrix. Some physiological and pathological cellular processes, such as morphogenesis and tumor growth, are known to exclusively occur in 3D cells (Berube et al., 2010). Because the 3D cells are more sensitive to toxicity, it is likely that the model better recapitulates an *in vivo* response. The 3D environment allows epithelial cells to polarize and differentiate into apical and baso-lateral surfaces (Berube et al., 2010). Past studies that have investigated differences between normal and asthmatic epithelium have found asthmatic epithelium to display differential expression of some genes and less differentiated phenotype (Stewart et al., 2011). Biomarkers relevant for PAH toxicity were evaluated in asthmatic and normal 3D HBEC treated with varying concentrations of BaP, DBC, and CTE.

Barrier Function/ Tight Junctions

The epithelial cell layer is the airway's first line of defense against pathogens and particles. It is also what dictates how the lung responds to infectious and noninfectious stimuli (Brune et al. 2015). Asthma causes chronic inflammation of the airway epithelium; diseases that cause inflammation in the lungs causes the epithelium to be more susceptible to damage. The barrier function integrity of the lung epithelium is dependent on tight junctions, which can be affected by lung inflammation (Wittekindt, 2017). Accumulation of ROS further decreases the level of tight junction proteins such as zona occludin (Chen et al. 2015). Previous research has

found that PAHs can disturb the cellular barrier function, causing increased permeability, inflammation, and oxidative stress of the airway epithelium.

Inflammation-based lung disease

Chronic obstructive pulmonary disease (COPD) and asthma have been linked to potential increased susceptibility to chemical pollutants based on common mechanisms of action.

Individuals with chronic obstructive pulmonary disease (COPD) have greater incidence of lung cancer (Stewart et al., 2011). Genetic predisposition implies that there is a connection between genetic susceptibility and disease; some individuals have clear genetic causes of COPD. A study found that exposure to high concentrations of BaP-equivalents is linked to increased risk of COPD. The main pathway these PAH effects were mediated through was the aryl hydrocarbon receptor pathway (Yang et al. 2016). PAH binding to the AhR causes transcriptional upregulation of genes, biotransformation, and differentiation (Dybing et al., 2013). A previous study has also found that PAHs have the ability to activate survival signaling kinases that increase the likelihood of survival for DNA-damaged cells (Dybing et al., 2013). ROS accumulation can lead to adverse effects contributing to the pathogenesis of COPD.

In the present study, we evaluated PAH toxicity in both normal and diseased (COPD/Asthmatic) donor primary human bronchial epithelial cells differentiated and cultured at the ALI. The goal of this study was to evaluate the response to PAH exposure between normal and diseased cells and their susceptibility to chemical insult. Our previous data suggests there may be differences in sensitivity between cells from healthy donors and asthmatic donors. Currently there is lack of information regarding the effects of PAHs in both normal and diseased 3D lung epithelial cells. To evaluate potential differences in PAH toxicity between normal and diseased cells, we utilized *in vitro* assays, microscopy, and computational approaches.

Materials and Methods

Chemicals and Reagents

Cell culture media and phosphate buffered saline (PBS) were provided by MatTek Corporation (Ashland, MA). Benzo[*a*]pyrene (CAS# 50-32-8) and dibenzo[*def,p*]chrysene (CAS# 189-64-0) were purchased from MRIGlobal (Kansas City, MO). Coal Tar Extract, SRM 1597a, (CTE) was purchased from the National Institute of Standards & Technology (Gaithersburg, MD). 2,7-Dichlorofluorescein (CAS# 4091-99-0) was purchased from Sigma Aldrich (St. Louis, MO). DNase I, TRIzol® reagent, Superscript® III First Strand Synthesis System, qPCR primers, and Pierce™ LDH Cytotoxicity Assay Kit were from Thermo Fisher Scientific (Waltham, MA). 2X SsoAdvanced™ Universal SYBER®Green Supermix was purchased from BioRad Laboratories, Inc. (Hercules, CA.)

Tissue culture and treatments

For 3D cell culture, primary HBEC from EpiAirway™ 100 were transferred to 6-well plates each containing 1 ml of assay medium. The tissues were equilibrated for 24 hours at 37°C, 5% CO₂ followed by a change of fresh medium prior to treatment administration. Inserts were washed using phosphate buffered solution (PBS, pH 7.4) and treated with benzo[*a*]pyrene (BaP), dibenzo[*def,p*]chrysene (DBC) or coal tar extract (CTE) at concentrations ranging 0.016-25.0 µg/cm in PBS with 1% DMSO on the apical surface for up to 48 hours. Apical washes and basal media were collected in clean, sterile tubes and stored at -80°C. At the end of each exposure regimen, the matrix and tissue from each well insert was carefully peeled away with forceps, placed in cryovials containing 0.5ml TRIzol® reagent and snap frozen in liquid nitrogen. Frozen tissues were stored at -80°C until further analysis.

For 2D cell culture, primary normal HBEC were expanded in media and subcultured on black-walled 96-well plates until cells were 85-100% confluent. Cells were exposed to benzo[a]pyrene (BaP), dibenzo[def,p]chrysene (DBC) or coal tar extract (CTE) at concentrations ranging 0.2-100 µg/ml in PBS with 1% DMSO and incubated for 24 hours at 37°C, 5% CO₂. After 24 hours, treatment and media solution were removed; media samples were stored at -20°C for future LDH assays. 20 µM 2,7-Dichlorofluorescein (DCFDA) in 2% DMSO was quickly transferred onto each well. Plates were immediately read on a BioTek Synergy HTX plate reader (Winooski, VT) to determine reactive oxygen species generation.

Transepithelial Electrical Resistance (TEER)

Transepithelial electrical resistance (TEER) was measured by using an EVOM2 Epithelial Volt-Ohm meter, World Precision Instruments (Sarasota, FL) to measure electrical resistance across the cell layer. The EVOM2 was calibrated prior to resistance measurements (ohms). In this study, TEER was measured at 0 hr and at 48 hr to determine the decrease in barrier integrity of PAH-treated samples compared to vehicle. Background resistance was corrected for by using an empty culture insert. Each PAH treatment had four culture inserts that were used for measurement. The background was subtracted from both time points 0 hr TEER and 48 hr TEER. TEER was calculated as the difference between 48 hr minus background and 0 hr minus background. Significance ($p < .05$) of the difference from the PBS/DMSO control was evaluated by one-way ANOVA with Dunnett's multiple testing correction.

Lactate Dehydrogenase Assay

A Pierce LDH Cytotoxicity Assay Kit and a standard operating protocol provided in the kit was used for reagent preparation. The cytotoxicity of normal and asthmatic donor cells treated with different PAH treatments (n=4) was assessed with the use of LDH Cytotoxicity

assay. LDH leakage into the basal media of the treated cells collected at 48 hr during TEER was measured to determine cytotoxicity. 50 µl of the supernatant was aliquoted into a new 96-well plate; 50 µl of reaction mixture was then aliquoted to each sample and incubated at room temperature for 30 minutes while protected from light. After 30 minutes, 50 µl of stop solution was added to each well and mixed. The absorbance was measured at 490 nm and 680 nm using a BioTek Synergy HTX plate reader (Winooski, VT) to determine LDH activity. The cytotoxicity was determined by subtracting the absorbance measured at 680 nm (background) from that of 490 nm. Significance ($p < .05$) of the difference from the PBS/DMSO control was evaluated by one-way ANOVA with Dunnett's multiple testing correction.

RNA extraction

Cells were harvested from HBEC and stored at -80°C. Total RNA extraction was performed using TRIzol® reagent per manufacturer's standard operating protocol. A BioTek Synergy HTX plate reader equipped with a Take3 Micro-Volume plate was used to quantify concentrations of RNA from samples.

Quantitative Polymerase Chain Reaction (qPCR)

A Superscript® III First Strand Synthesis System was used to synthesize cDNA following the manufacturer's standard operating protocol. Reactions were diluted 1:10 with ultrapure water, then aliquoted to 40, 40, 20 µl per tube. cDNA was stored at -80°C until used for qPCR. A BioRad Laboratories, Inc. (Hercules, CA.) CFX96 Touch™ Real-Time PCR Detection System was used to run total volume 10 µl qPCR reactions. CLN1, CLN4, TJP2, GJA1, CYP1A1, CYP1B1, and NQO1 primers were used. Each reaction contained 2 µl cDNA, 0.6 µl forward primer, 0.6 µl reverse primer, 5.0 µl 2X SsoAdvanced™ Universal SYBER®Green Supermix, and 1.8 µl nuclease-free water. The thermocycler was programmed for 1 cycle 95 °C for 1 min

initial denaturing, 40 cycles 95 °C for 15 s denaturing, 60 °C for 30 s annealing/elongation, and a melt curve 65–95 °C/0.5° per 5 s for validating single product amplification. Relative gene expression was calculated using the $\Delta\Delta C_t$ comparative method and normalized to the housekeeping gene *peptidylpropyl isomerase A (PPIA)*. Treatments significantly regulated from PBS/DMSO control ($p < 0.05$) were identified by one-way ANOVA with Dunnett's multiple testing correction.

Immunofluorescence

Double immunofluorescence labeling was done with monoclonal antibodies from Cell Signaling Technology, CLDN-4 and ZO-2. The HBEC were fixed in methanol/acetone and immunostained with A-Ms 647 and a-Rab 488 over the course of two days. They were then mounted on slides for imaging. A Zeiss LSM 780 NLO Confocal Microscope system, an argon laser, 40x oil lens, and DAPI was used to image stained cells. The software Zeiss Zen was then used for digital imaging and processing of images. The confocal microscope was used to visualize specific protein markers and three-dimensional structure of epithelial cell junctions in the cell model.

Process Analysis

RNAseq data from normal cells treated with concentrations of BaP of 10, 100, 500 $\mu\text{g/ml}$ was transformed by \log_{10} and uploaded into MultiExperiment Viewer (MeV) version 10.2 (Howe et al., 2011). The data was analyzed using K-means ten to cluster genes using Pearson Correlation. Centroid graphs were evaluated to determine positive and negative dose responsive clusters. Two clusters that demonstrated a positive dose response and two clusters that demonstrated a negative dose response were saved. All four clusters were uploaded onto commercial software MetaCore version 20.1 (<http://www.genego.com/>). The dataset was

analyzed using MetaCore's one-click analysis tool. The MetaCore clusters were downloaded and loaded into MeV to perform hierarchical clustering of each cluster group. The heat map was constructed using default MeV settings.

Benchmark dose modeling

BaP 10, 100, 500 $\mu\text{g/ml}$ RNAseq data was imported into BMDEExpress (Version 2.3) and a benchmark dose analysis was run. The imported RNAseq dataset was analyzed using the EPA BMDS Models (parametric); the default settings for benchmark dose analysis was used (Yang, Allen and Thomas, 2007). The values from benchmark dose were used to perform a functional classification analysis, specifically a defined category analysis. The defined category analysis allows the user to define special categories. Process networks for the analysis were selected using the criteria top 3 significant per process network category on MetaCore. The process networks were downloaded from MetaCore and the Probe Map file and Category Map file were created based on the obtained process networks. The input files contained NCBI Entrez Gene identifiers and Ensembl IDs obtained from Bioinformatics Resource Manager (Brown et al., 2019). The Probe Map file contained Ensembl IDs in the first column labeled probe identifiers and Entrez Gene identifiers in the second column labeled gene identifiers. The Category Map file had the category number in the first column labeled category identifiers, the process networks named in the second column labeled category name, and the Entrez Gene identifiers in the third column labeled category component. The category number remained constant for a process network. The defined category analysis was run using the user inputted Probe Map and Category Map files and default category analysis setup. The median benchmark dose of the selected process networks were evaluated to determine the most sensitive process networks.

Results

To evaluate cytotoxicity in 3D HBEC, LDH leakage was measured after 48 h exposure to BaP, DBC, and CTE in basal medium (Fig. 1A and B). Normal HBEC exposed to the PAHs showed non-significant trend towards increased cytotoxicity after DBC treatment with increasing concentration. BaP and CTE treated cells showed no increase in cytotoxicity compared to control at any concentration. No chemical treatments of normal cells showed significant leakage from control. In asthmatic HBEC, DBC resulted in an increase in LDH leakage that was dose dependent. The highest concentration of DBC in asthmatic HBEC showed a significant leakage ($p < 0.01$) from the vehicle control. There was no dose response evident from asthmatic cells treated with BaP and CTE. There was a trend of increased leakage at high concentrations. Overall, there were no clear cytotoxicity differences identified between normal and asthmatic cells by the LDH assay.

Normal and asthmatic 3D HBEC were further assessed for potential differences in PAH sensitivity by measuring barrier function integrity (Fig. 2A and B). TEER was measured at 48 h after chemical treatment to determine barrier function integrity. Normal cells exposed to DBC showed a dose-dependent increase in TEER measurements, with a statistically significant increase at the highest concentration. CTE and DBC treated asthmatic cells had no trend of barrier function related to dose. BaP and CTE exposed cells did not result in barrier integrity differences between normal and asthmatic cells.

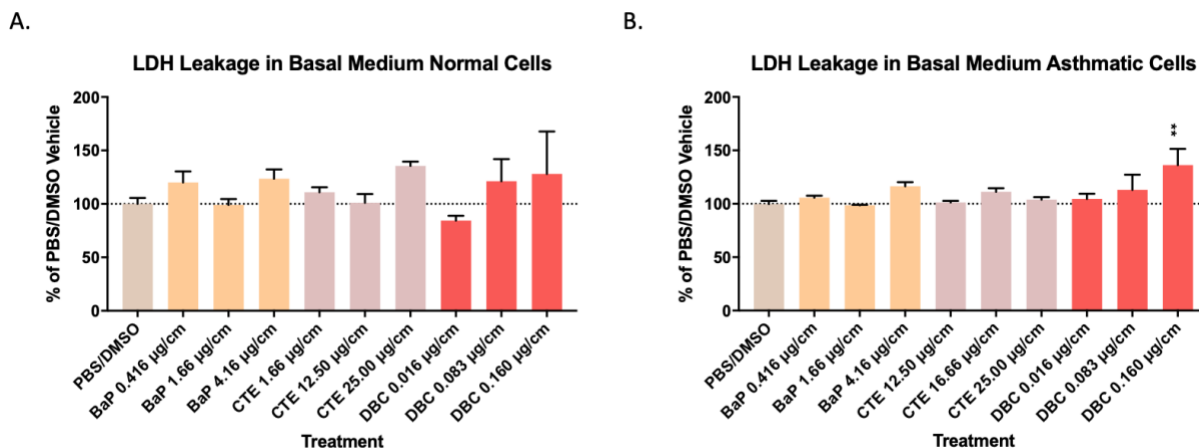


Figure 1. Cytotoxicity in HBEC after 48 hr exposures to PAHs. (A-B) Cytotoxicity was measured by lactate dehydrogenase (LDH) leakage into the basal media of the chemically treated cells collected at 48 h. *Indicates a significant difference from vehicle control (* $p < 0.05$, ** $p < 0.01$; one-way ANOVA with Dunnett's multiple testing correction).

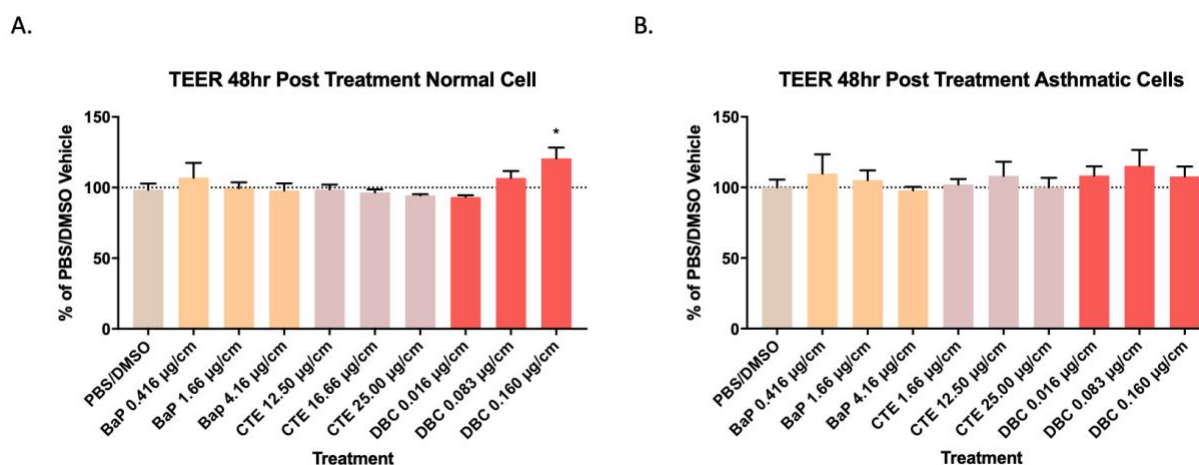


Figure 2. Barrier function and integrity of PAH treated HBEC samples. (A-B) Transepithelial electrical resistance (TEER) was measured at 0 h and 48 h after PAH treatment. Decreases in barrier integrity of BaP, DBC, and CTE treated samples were compared to vehicle control. *Indicates a significant difference from vehicle control (* $p < 0.05$, ** $p < 0.01$; one-way ANOVA with Dunnett's multiple testing correction).

To further evaluate barrier function integrity, biomarkers claudin 1 (CLN1), claudin 4 (CLN4), tight junction protein 2 (TJP2), and gap junction 1 (GJA1) were chosen because these genes make up gap junction and tight junction proteins. Barrier function genes expressed a

pattern of downregulation across all PAHs exposures. Gene expression for barrier function genes in diseased cells had greater downregulation than normal cells (Fig 3). Barrier function genes were significantly regulated by PAH exposure in diseased cells. In normal HBEC, no significant changes in gene expression were detected for CLN1, CLN4, TJP2 and GJA1 across all three chemicals. However diseased cells showed significant downregulation for CLN1 and CLN4. Both normal and diseased cells did not have significant gene expression for TJP2. Overall, exposure to BAP, DBC, and CTE resulted in a similar downregulation of the barrier junction genes evaluated, with some genes exhibiting greater sensitivity in diseased cells.

Metabolizing genes Cytochrome P450 Family 1 Subfamily A Member 1 (CYP1A1), Cytochrome P450 Family 1 Subfamily B Member 1 (CYP1B1), and NAD(P)H Quinone Dehydrogenase 1 (NQO1) were also chosen for qPCR. For this category of genes, normal cells exhibited greater upregulation in response to PAH treatment than diseased cells (Fig 3). CYP1A1 and CYP1B1 had similar patterns of gene expression across treatments for both normal and diseased cells. Gene expression for NQO1 for diseased cells was downregulated. NQO1 gene expression for normal cells exposed to BaP exhibited upregulation. For cells exposed to DBC, diseased cells exposed to DBC had significantly ($p < 0.05$) greater downregulation, which supports chemical-specific differences in response. CTE exposed normal and diseased cells had no significant expression with NQO1. In metabolizing genes, there are clear differences in PAH-induced gene regulation between normal and diseased cells.

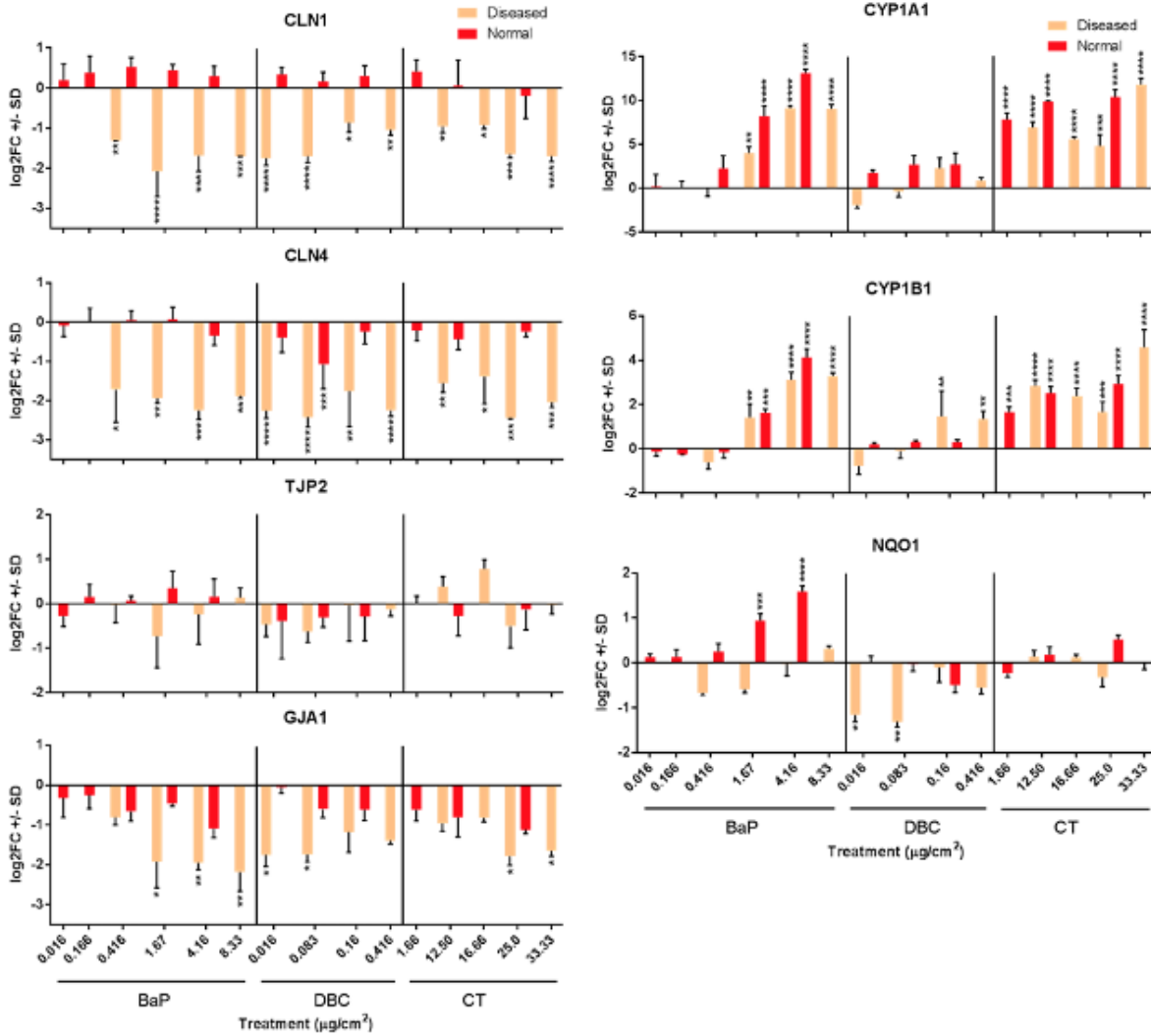


Figure 3. Barrier function and metabolizing gene expression in HBEC. HBEC were exposed on the apical side with benzo[a]pyrene (BaP) (0.2-50 ug/mL), dibenzo[def,p]chrysene (DBC) (0.2-2 ug/mL) and coal tar extract (CTE) (0.02-0.3 ug/mL) in PBS with 1% DMSO. *Indicates significance from PBS/DMSO control (* p <0.05, ** p <0.01, *** p <0.001).

Barrier proteins in normal 3D HBEC were visualized by double immunofluorescence labelling and confocal microscopy after cells were treated for 48 hrs with BAP, DBC and CTE compared to control cells (Fig 4). Monoclonal antibodies for CLN4 and ZO-2 were used for protein detection. BaP and DBC exposure did not result in observed delocalization in barrier proteins. BaP and DBC treated cells showed that Zo-2 had colocalized with CLN4. There was

low specificity and high background surrounding the cell bodies. Zo-2 had very little specificity in CTE cells, which made it difficult to see the cells. Zo-2 and CLN4 colocalization in CTE-treated cells was not observed; however, it is unclear whether this was due to sample preparation where ZO-2 detection was not as prominent, or potentially due to chemical-related delocalization. ZO-2 and CLN4 were not defined in the periphery of the CTE cells. Images obtained by confocal microscopy of normal cells showed that there may be an effect on barrier function in cells stained with Zo-2 and CLN4.

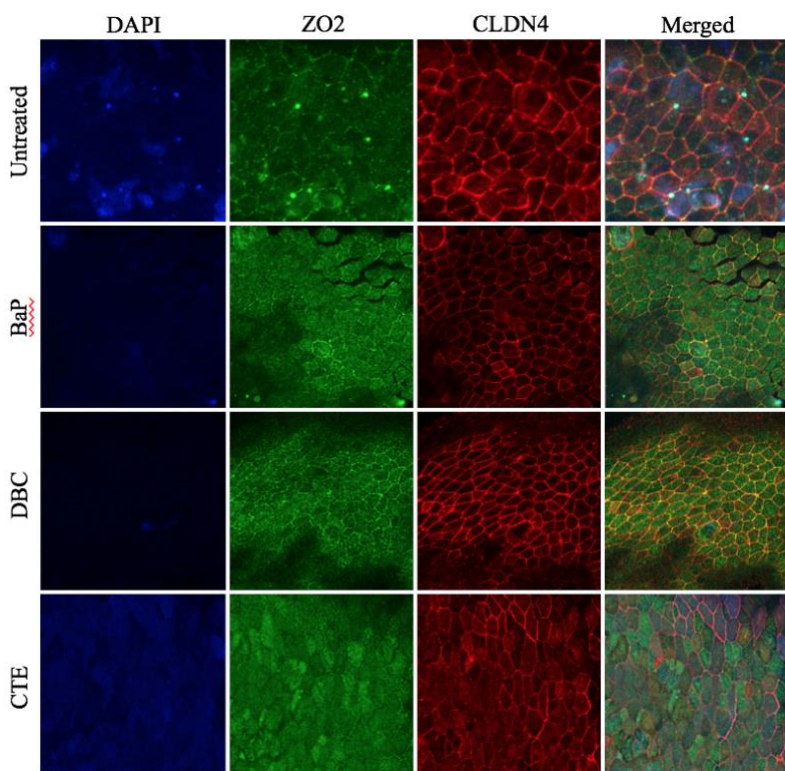


Figure 4. Visualization of barrier function in normal cells. 3D normal HBEC treated with either benzo[a]pyrene (BaP), dibenzo[def,p]chrysene (DBC) or coal tar extract (CTE) were stained with DAPI and labeled using monoclonal antibodies, Zona occludins-2 (ZO2) and Claudin-4 (CLDN4).

Oxidative stress was measured as a potential mechanism for toxicity by PAHs through measurements of DCFDA in normal and asthmatic cells cultured in 2D. Cells were treated with dose ranges of BaP, DBC, and CTE to determine if there were any chemical dependent differences in intracellular reactive oxygen species (ROS) generation between normal and diseased cells. Overall, there is a significant dose dependent increase in ROS generation from

exposure to all three PAHs in both normal and diseased cells. BaP treated diseased cells had significantly greater intracellular ROS generation than normal cells ($p < 0.05$) in doses 10, 20, and 80 $\mu\text{g}/\text{mL}$ (Fig 5A). All doses of BaP consistently resulted in greater ROS generation in diseased cells. Cells treated with DBC did not have significant differences in ROS generation between normal and diseased cells (Fig 5B). However, a dose dependent increase was still evident in DBC treated cells. CTE treated cells produced the greatest amount of ROS in comparison to other chemicals. Normal cells treated with CTE doses 40 and 100 $\mu\text{g}/\text{mL}$ had significantly higher ROS generation than diseased cells ($p < 0.05$) (Fig 5C). We have observed a trend of greater ROS generation in CTE treated normal cells than diseased at doses 10-100 $\mu\text{g}/\text{mL}$. In cells treated with BaP, we observed greater sensitivity for PAH induced ROS generation; whereas exposure to CTE had a decrease in sensitivity in diseased cells. There was no difference in sensitivity identified in DBC treated cells. We found that BaP exposed diseased cells were more sensitive than normal, DBC treated cells had the same sensitivity in normal and diseased, and CTE treated normal cells were more sensitive. These results support that chemical sensitivity between donors is also chemical specific and possibly mechanism specific.

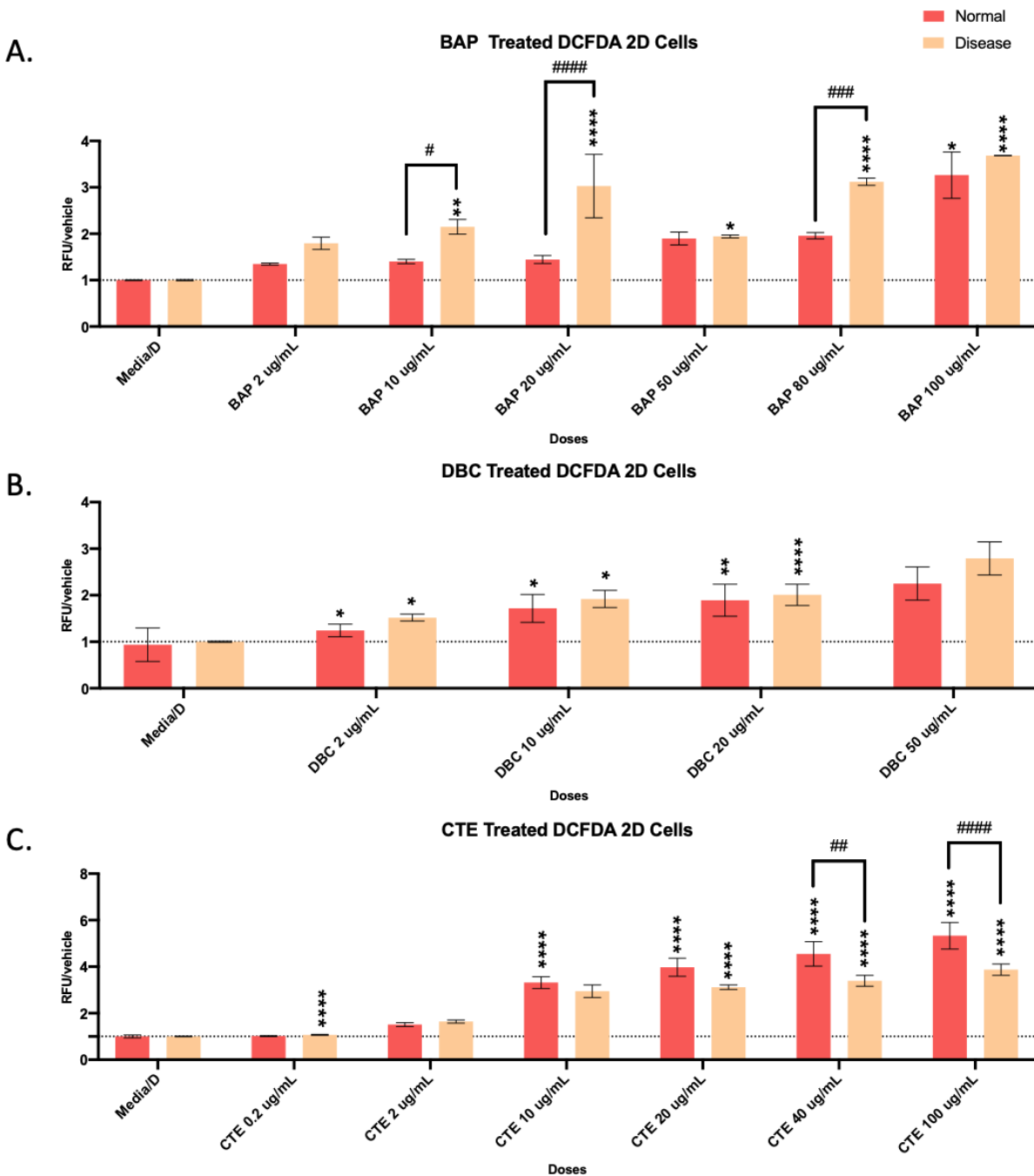


Figure 5. Intracellular Reactive Oxygen Species Generation in 2D Cells. 2D DCFDA normal and diseased cells were treated with varying doses of benzo[a]pyrene (BaP), dibenzo[def,p]chrysene (DBC) or coal tar extract (CTE). *Indicates significance from PBS/DMSO control (* $p < 0.05$, ** $p < 0.01$, *** $p < 0.001$, **** $p < 0.0001$) one-way ANOVA with Dunnett's multiple testing correction. #Indicates significance between normal and diseased cells (# $p < 0.05$, ## $p < 0.01$, ### $p < 0.001$, #### $p < 0.0001$) one-way ANOVA.

To evaluate gene changes sensitive to dose-response treatment by BaP in 3D HBEC, K-means 10 clustering was performed using genes significantly regulated by BAP compared to control treatment ($q < 0.05$). Global gene expression was previously evaluated by RNAseq in 3D HBEC 48 hr after treatment with a dose-response of BAP (10-500 $\mu\text{g/ml}$) (Chang et al., 2020). We focused on two clusters that showed decreasing trend in gene regulation with dose (Fig 6A) and consistent increase in gene regulation with dose (Fig 6B) after BAP treatment. Hierarchical clustering of each cluster of genes (Fig 6C and D) was performed to further examine pathways associated with gene clusters. Heatmaps supported that there are different processes that are highlighted as dose dependent. Cell adhesion and oxidative stress (protein folding) were downregulated with increasing BAP dose (Fig 6C). Inflammation and apoptosis processes were increased with BAP dose (Fig 6D).

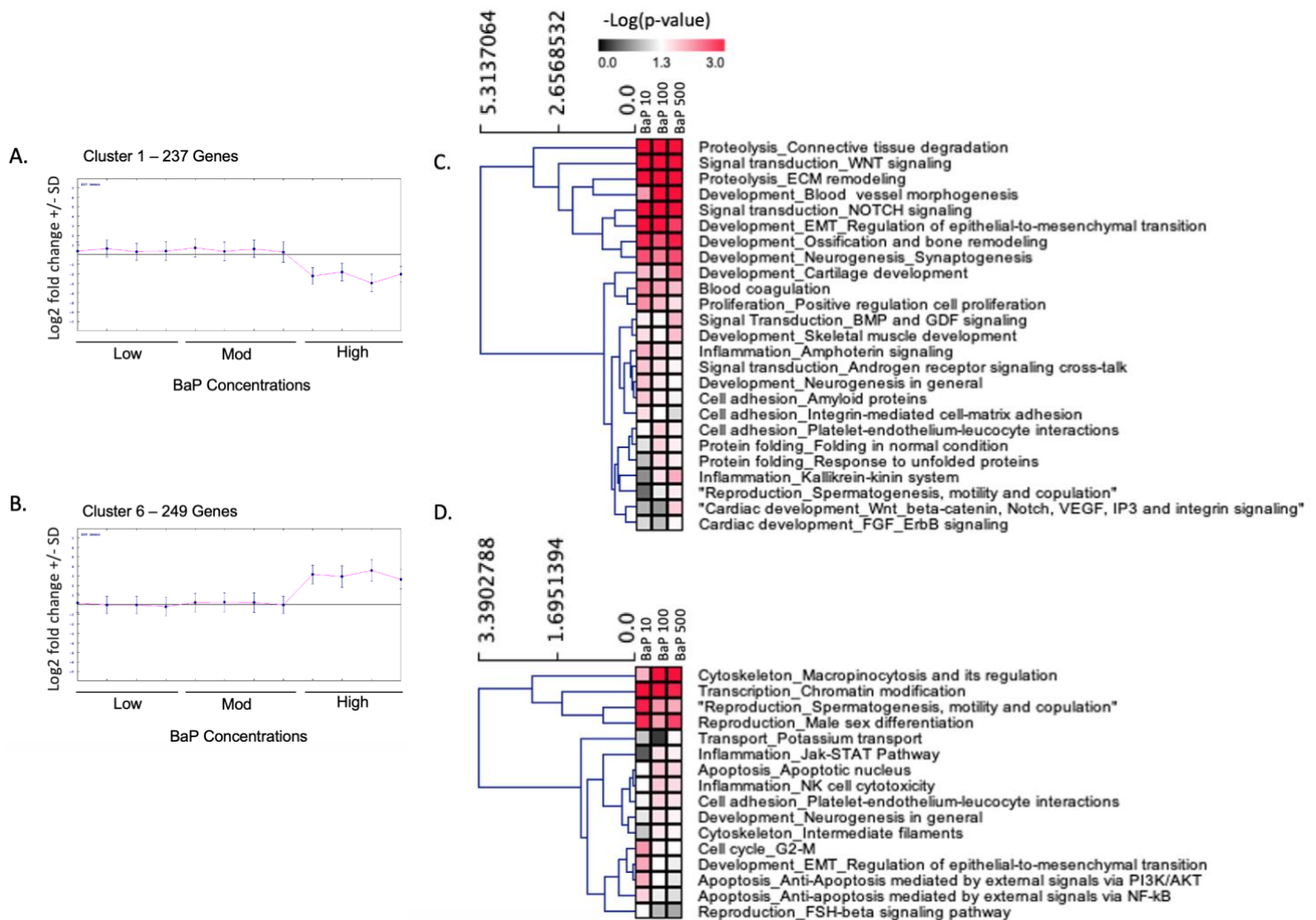


Figure 6. K-means 10 clustering and hierarchical clustering. (A-B) Centroid graphs produced from K-means 10 clustering of BaP RNAseq data. BaP dose response data was obtained at concentrations BaP 10 µg/mL (low), 100 µg/mL (mod) and 500 µg/mL (high). (C-D) Hierarchical clustering heat maps produced using the genes identified in K-means 10 clustering as dose responsive.

In addition to K-means clustering, we also performed benchmark dose modeling (BMD) of the significant RNAseq data to more quantitatively identify genes and pathways that are sensitive to dose-response treatment by BaP in 3D HBEC. BMD analyses was used with user-defined functional classification analysis using the top 30 prioritized pathways. The ten most sensitive pathways were identified by ranking BMD medians; the lowest BMD medians are most sensitive (Fig 7A). The most sensitive gene set to BaP regulation was regulation of cytoskeleton

rearrangement; which had 84 genes that passed all filters (Fig 7B). Within regulation of cytoskeleton rearrangement; the three most sensitive genes were identified to be Vav Guanine Nucleotide Exchange Factor 2 (*VAV2*), Adducin 1 (*ADD1*) and Enah/Vasp-Like (*EVL*) (Fig 7C). The other pathways that were more sensitive to BaP gene regulation are two DNA damage pathways, another cytoskeleton pathway, and a transcription pathway (Fig 7B). Biological functions that may be sensitive to BaP dose response were identified using a pathway category-level analysis using the results from the functional classification analysis. The BMD medians per pathway category were averaged to determine the most sensitive pathway categories to BaP gene regulation. The most sensitive pathway categories were Cytoskeleton (avg BMD median = 240.60 ug/mL), Regulation of metabolism (avg BMD 247.88 ug/mL), and Protein folding (avg BMD media = 252.99 ug/mL). The least sensitive pathway categories to BaP gene regulation were Chemotaxis (avg BMD median = 445.43 ug/mL) and Blood (avg BMD median = 441.96 ug/mL).

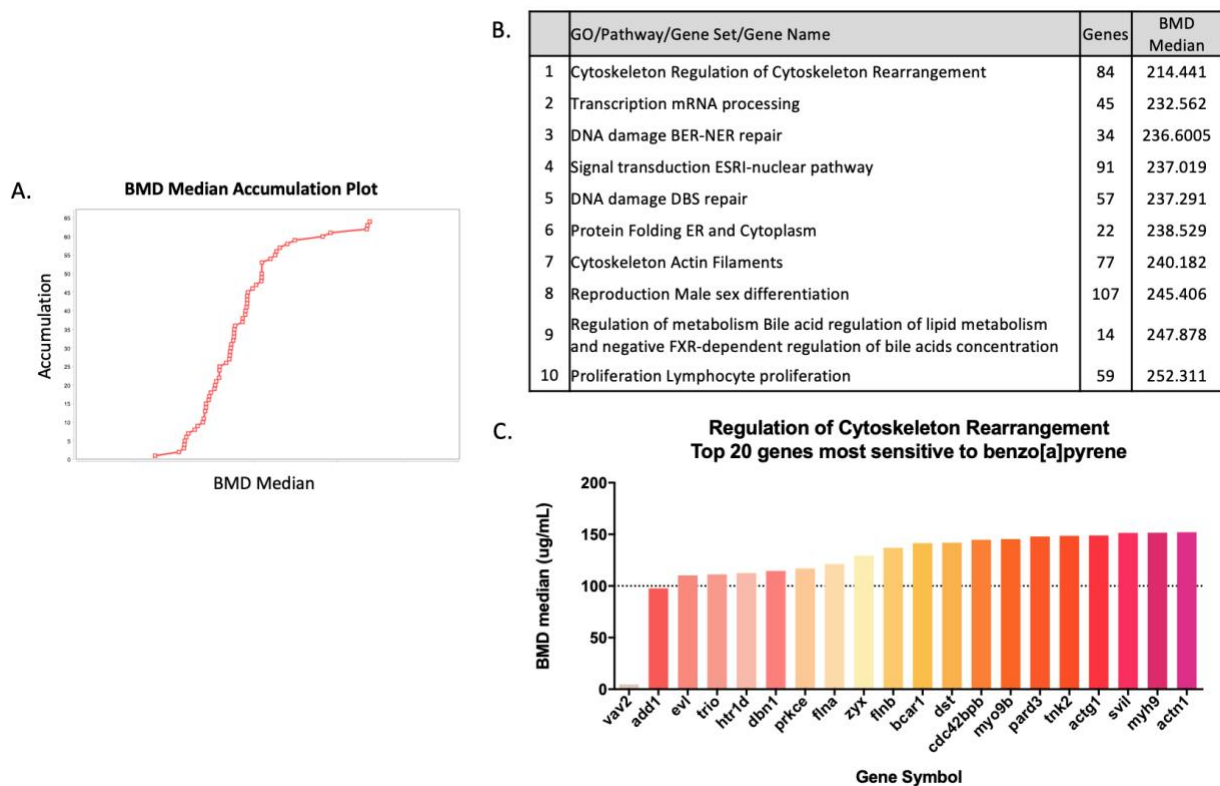


Figure 7. Transcriptomic dose-response modelling of top 3 most significantly enriched pathways per pathway category. (A) The most sensitive pathways to BaP regulation were identified using BMD analyses and user-defined functional classification analysis. The lowest BMD median and was the most sensitive to BaP gene regulation. (B) The 10 most sensitive pathways include pathway categories Cytoskeleton, Transcription, DNA damage, and protein folding. (C) The 20 most sensitive genes within the regulation of cytoskeleton rearrangement pathway were graphed sorted by their BMD median (ascending) to determine most sensitive genes within the pathway. The most sensitive gene is VAV2.

Discussion (1,811/1,500)

Certain polycyclic aromatic hydrocarbons are found to be procarcinogenic and carcinogenic, with varying levels of carcinogenic potency (Siddens et al., 2012). PAH mechanisms of toxicity, including oxidative stress and barrier function integrity, need to be further investigated in normal and asthmatic human bronchial epithelial cells to determine the contribution of disease state to possible increased susceptibility to lung disease and cancer. In the

present study, we utilized a 3D, differentiated human *in vitro* bronchial epithelial model to assess potential differences between normal and diseased donor cells in response to PAH exposure.

PAH-related changes in barrier integrity

Functional gene expression assays and confocal microscopy were used to evaluate barrier function integrity in normal and asthmatic HBECs treated with various PAH treatments. Studies have found that PAHs induce barrier dysfunction; promoting destruction of membrane integrity and permeability (Dai et al., 2016). Barrier dysfunction has been involved in the pathogenesis of many pathological conditions in pulmonary tissues. Disruption of intercellular tight junctions and gap junctions can disturb lung tissue homeostasis leading to the onset of asthma and lung cancer (Cao et al., 2015). Barrier function is evaluated as a potential predictor of toxicity due to its disruption caused by oxidative stress and inflammation and association with COPDs. PAH treatment has been correlated to reduction in TEER values and induction of cellular toxicity (Cao et al., 2015).

Trans-epithelial electrical resistance (TEER) was measured to determine the integrity and permeability of the tight junctions. We found that normal and asthmatic cells both had a reduction in TEER as PAH exposure increased. At the highest concentration of DBC exposure, normal cells had a significantly increased TEER measurement ($p < 0.05$). These results do not coincide with a study that previously found a loss of cell barrier integrity at high concentrations of BaP and DBC exposure in 3D HBEC (Chang et al., 2019). Barrier proteins were visualized in normal 3D HBEC to assess tight junction integrity. We found no evidence of barrier disruption in normal cells but may be evident in diseased cells. There is a possible treatment effect in cells treated with CTE. Gap junction marker GJA1 was down-regulated by all treatments; at some concentrations, diseased cells were significantly down-regulated. Diseased cells were more

downregulated than normal cells across all barrier function genes, CLN1, CLN4, TJP2, and GJA1. Differences between normal and diseased HBEC suggest that gene expression may be more sensitive than TEER. Previous studies done in animal models found that increased production of inflammatory mediators, including cytokines and reactive oxygen species, results in the disruption of the epithelial barrier causing the destabilization of tight junctions (Rao, 2018). While it is difficult to clearly define the relationship between inflammation and lung epithelial barrier; these results suggest that diseased donor cells exposed to certain PAHs may be more susceptible to barrier disruption. The reduction in epithelial barrier function as measured by TEER and qPCR, and visualized by confocal microscopy supports barrier disruption as a possible mechanism of action for PAH toxicity that may be altered by a disease state.

Intracellular ROS generation

There are different pathways for mechanisms of activation of carcinogenic PAHs (Dybing et al., 2013). Parental PAH molecules are procarcinogens that get transformed into carcinogenic metabolites. CYPs and other metabolic enzymes generally metabolize PAHs into phenols, catechols, and quinones. This results in the formation of reactive o-quinones, epoxides, and radical cations that can all react with DNA to produce DNA and protein adducts in cells (Moorthy, Chu and Carlin, 2015). Reactive metabolites of PAHs can also cause an increase in reactive oxygen species levels; reactive oxygen species affects DNA, lipids and proteins (Wilk et al., 2013). The elevation of reactive oxygen species contributes to cancer etiology.

Results of gene expression for CYP1A1 and CYP1B1 had similar trends of upregulation for normal and asthmatic cells. However, CYP1A1 was more upregulated than CYP1B1 and NQO1. Because of the greater upregulation, CYP1A1 was found to be a more sensitive gene to serve as a biomarker for BaP exposure, regardless of disease state. CYP1A1, a PAH-

metabolizing cytochrome p450 enzyme, is regulated by the aryl hydrocarbon receptor; individuals with high expression of CYP1A1 are at increased risk of developing COPD (Wang et al., 2015). Studies have found a relationship between levels of aryl hydrocarbon hydroxylase, CYP1A1 dependent enzyme activity, and BaP-DNA adducts in lung tissue of tobacco smokers (Anttila et al., 2001). CYP1A1 gene polymorphisms have been found to be associated with higher COPD risk, further supporting the potential role of CYP1A1 in COPD development. Gene expression data showed that PAH treatments BaP and CTE induced CYP1A1 and 1B1 more than DBC treated cells. These results suggest that BaP and CTE may cause CYP1A1 and 1B1 to have differing mechanisms in metabolism than DBC, which supports differences between the PAHs identified previously (Chang et al., 2019). NQO1 was significantly upregulated for normal cells exposed to BaP and downregulated across all treatments in diseased cells. NQO1 is an antioxidant enzyme that plays a role in the reduction of quinone levels thereby decreasing the generation of reactive oxygen species (Dinkova-Kostova and Talalay, 2010). The upregulation of NQO1 was not observed in normal cells exposed to DBC and CTE. The upregulation of NQO1 in BaP treated normal cells suggests that normal cells may have differences in ROS antioxidant response. These results are supported by a previous study that found BaP to upregulate antioxidant genes and DBC to downregulate them (Chang et al., 2019).

Increased production of ROS causes oxidative stress that can cause cellular structure and function damage. Our results from DCFDA cellular ROS detection assay for BaP and DBC exposed HBEC support numerous studies that have found higher oxidative stress in those with COPD (Boukhenouna 2018; Kirkham and Barnes 2013; Rahman 2005). COPD is characterized by chronic inflammation; cigarette smokers also experience high oxidative stress due to high concentration of oxidants and free radicals (Boukhenouna, 2018). Cells from donors of a

diseased state produced significantly greater intracellular ROS than normal cells for BaP treated cells; previous studies have found oxidant and antioxidant molecule expression levels are imbalanced in COPD patients (McGuinness and Sapey, 2017). Diseased cells were more sensitive to BaP exposure than normal; diseased donors have greater risk of COPD than normal donors. Cells that are altered by COPD effect the antioxidant defense systems that remove ROS (Boukhenouna, 2018). Diseased cells displayed less sensitivity to CTE exposure than normal cells. Crude coal tar has been used medicinally for its anti-inflammatory properties; more specifically, it has been used as a topical to treat chronic inflammatory skin conditions such as psoriasis (Arbiser et al., 2006). The DCFDA assay results suggest that greater caution should be taken towards CTE usage as an anti-inflammatory because exposure in both cell types resulted in elevated intracellular ROS, although normal cells had greater sensitivity to CTE exposure. Our assessments of ROS generation combined with barrier and metabolizing gene expression suggests there may be differences in sensitivity and that diseased cells have greater susceptibility to chemical insult. Individuals with preexisting respiratory conditions may therefore be at greater risk of developing COPD when exposed to air pollutants such as PAHs.

Toxicogenomic Biomarker Identification Through Transcriptomic Benchmark Dose Modelling

Vector quantization and transcriptomic dose-response modelling were used to identify sensitive and dose-responsive pathways to BaP gene regulation. K-means 10 clustering and hierarchical clustering found the “Proteolysis connective tissue degradation” pathway to be most negative dose-responsive to BaP gene regulation. Hierarchical clustering of a positive dose-responsive gene cluster found “Cytoskeleton micropinocytosis and its regulation” pathway to be most sensitive. The pathways that were included in the benchmark dose analysis were the top 30

previously prioritized process networks and the top 3 most significant process networks from each category. These pathways were prioritized with the goal of identifying relevant geneset classifier pathways to BaP dose-responsiveness. Pathways related to oxidative stress, inflammation, and barrier function were not prioritized in this analysis.

A previous study has identified processes that have dose-dependent effects of Benzo[a]pyrene diol epoxide (BPDE) on gene expression. The genesets modelled at BMD10 found the most sensitive pathway to be “Regulation of cytoskeleton rearrangement”, which supports previous findings that cytoskeleton organization processes are downregulated by BaP exposure. We have also modelled genesets at BMD5 and found that cell cycle processes are sensitive to BaP. The identified BaP-sensitive pathway genesets identified in this study support the literature study in normal human lung fibroblasts that found inflammatory and immune response processes to be upregulated at high concentrations and cell cycle and intracellular organization processes to be downregulated at all concentrations of BPDE (Dreij, 2010). BPDE exposure significantly activates genes that are involved in cell proliferation and the cell cycle (Dreij, 2010). Identification of genes modelled to be most sensitive to BaP dose can be used in future studies that evaluate differences in susceptibility to chemical injury due to PAHs between HBEC from diseased and healthy donors.

Limitations

This study aimed to identify differences in sensitivity to toxicity between normal and asthmatic human bronchial epithelial cells. The cells were cultured in 3D air-liquid interface and treated with varying concentrations of PAHs. Due to solubility issues, not all concentrations of PAH exposure were applied to both normal and asthmatic cells. At some levels of PAH exposure, a direct comparison between normal and diseased could not be made. This study did

not reflect the real toxicity associated with complex mixtures since PAH exposure was done in isolation. Cells were also exposed to PAHs through pipetting solutions on apical side, instead of through vaporized compounds in *in vitro* exposure chambers. In the environment, PAH exposure often occurs in mixtures (Bláha et al., 2002). Mixtures of PAHs can modulate the behavior and potency of singular PAHs (Tilton et al., 2015). TEER and LDH were measured at 48 hours after exposure; only the initial response to PAH exposure was measured. *In vivo*, PAH exposure would be chronic. However, in this study comparisons between the effects of PAH exposure in normal and asthmatic cells cannot be concluded for chronic exposure. The changes of toxicity, effect on barrier function and cytotoxicity following exposure were not evaluated.

Future directions

Through identification and validation of sensitive gene biomarkers, we hope to develop additional biomarkers for use in future comparisons of cells of various health and disease states. Transcriptional biomarkers identified from transcriptomic dose-response modelling and benchmark dose modelling can be used to identify further gene expression differences between normal and asthmatic HBEC through real-time qPCR.

Potential directions for future analysis include examining interleukin 13 induced phenotype in comparison to normal and asthmatic cells. Interleukin 13 (IL-13) is a known mediator of allergic inflammation and different diseases, including asthma. IL-13 is involved in the regulation of airway inflammation and mucous production. miRNA are important post-transcriptional regulator molecules. miRNAs could be examined in BaP treated normal and diseased cells as well as normal cells treated with IL-13 to induce an asthmatic phenotype for comparison. The benefit of using IL-13 on cells is that IL-13 can be induced in the same donor cells normal cells. CYP1A1 gene polymorphisms have been linked to greater risk of COPD. 3D

cell cultures could be genotyped from different donor cells to evaluate different polymorphisms. The same endpoints as evaluated in this study could be used – barrier function, ROS generation, and metabolizing enzyme differences in sensitivity.

Another potential direction is to do further comparisons of normal and diseased cells in 2D and 3D HBEC models and evaluate differences in sensitivity between the cells and the different models. The findings of this study support recent research that people with underlying respiratory illnesses, such as asthma may have differing susceptibilities to environmental pollutants. Therefore, there is a need for more studies to be done investigating differences in sensitivity to air pollution between normal and diseased cells.

References

- Anttila S, Tuominen P, Hirvonen A, Nurminen M, Karjalainen A, Hankinson O, Elovaara E. 2001. CYP1A1 levels in lung tissue of tobacco smokers and polymorphisms of CYP1A1 and aromatic hydrocarbon receptor. *Pharmacogenetics*. 11(6):501–509. doi:[10.1097/00008571-200108000-00005](https://doi.org/10.1097/00008571-200108000-00005).
- Arbiser JL, Govindarajan B, Battle TE, Lynch R, Frank DA, Ushio-Fukai M, Perry BN, Stern DF, Bowden GT, Liu A, et al. 2006. Carbazole is a naturally occurring inhibitor of angiogenesis and inflammation isolated from antipsoriatic coal tar. *J Invest Dermatol*. 126(6):1396–1402. doi:[10.1038/sj.jid.5700276](https://doi.org/10.1038/sj.jid.5700276).
- BéruBé K, Pitt A, Hayden P, Prytherch Z, Job C. 2010. Filter-well technology for advanced three-dimensional cell culture: perspectives for respiratory research. *Altern Lab Anim*. 38(1_suppl):49–65. doi:[10.1177/026119291003801S04](https://doi.org/10.1177/026119291003801S04).
- Boukhenouna S, Wilson MA, Bahmed K, Kosmider B. 2018. Reactive oxygen species in chronic obstructive pulmonary disease. *Oxid Med Cell Longev*. 2018. doi:[10.1155/2018/5730395](https://doi.org/10.1155/2018/5730395).
- Brown J, Phillips AR, Lewis DA, Mans M-A, Chang Y, Tanguay RL, Peterson ES, Waters KM, Tilton SC. 2019. Bioinformatics Resource Manager: a systems biology web tool for microRNA and omics data integration. *BMC Bioinformatics*. 20(1):255. doi:[10.1186/s12859-019-2805-6](https://doi.org/10.1186/s12859-019-2805-6).
- Brune K, Frank J, Schwingshackl A, Finigan J, Sidhaye VK. 2015. Pulmonary epithelial barrier function: some new players and mechanisms. *Am J Physiol Lung Cell Mol Physiol*. 308(8):L731–L745. doi:[10.1152/ajplung.00309.2014](https://doi.org/10.1152/ajplung.00309.2014).
- Cao X, Lin H, Muskhelishvili L, Latendresse J, Richter P, Heflich RH. 2015. Tight junction disruption by cadmium in an in vitro human airway tissue model. *Respir Res*. 16(1). doi:[10.1186/s12931-015-0191-9](https://doi.org/10.1186/s12931-015-0191-9).
- Chang Y, Siddens LK, Heine LK, Sampson DA, Yu Z, Fischer KA, Löhr CV, Tilton SC. 2019. Comparative mechanisms of PAH toxicity by benzo[a]pyrene and dibenzo[def,p]chrysene in primary human bronchial epithelial cells cultured at air-liquid interface. *Toxicol Appl Pharmacol*. 379:114644. doi:[10.1016/j.taap.2019.114644](https://doi.org/10.1016/j.taap.2019.114644).
- Chen M, Yang T, Meng X, Sun T. 2015. Azithromycin attenuates cigarette smoke extract-induced oxidative stress injury in human alveolar epithelial cells. *Molecular Medicine Reports*. 11(5):3414–3422. doi:[10.3892/mmr.2015.3226](https://doi.org/10.3892/mmr.2015.3226).
- Dai J, Sun C, Yao Z, Chen W, Yu L, Long M. 2016. Exposure to concentrated ambient fine particulate matter disrupts vascular endothelial cell barrier function via the IL-6/HIF-1 α signaling pathway. *FEBS Open Bio*. 6(7):720–728. doi:[10.1002/2211-5463.12077](https://doi.org/10.1002/2211-5463.12077).
- Dinkova-Kostova AT, Talalay P. 2010. NAD(P)H:quinone acceptor oxidoreductase 1 (NQO1), a multifunctional antioxidant enzyme and exceptionally versatile cytoprotector. *Arch Biochem Biophys*. 501(1):116–123. doi:[10.1016/j.abb.2010.03.019](https://doi.org/10.1016/j.abb.2010.03.019).
- Dreij K, Rhrissorakrai K, Gunsalus KC, Geacintov NE, Scicchitano DA. 2010. Benzo[a]pyrene diol epoxide stimulates an inflammatory response in normal human lung fibroblasts through a p53 and JNK mediated pathway. *Carcinogenesis*. 31(6):1149–1157. doi:[10.1093/carcin/bgq073](https://doi.org/10.1093/carcin/bgq073).
- Dybing E, Schwarze PE, Nafstad P, Victorin K, Penning TM. Chapter 7. Polycyclic aromatic hydrocarbons in ambient air and cancer. In: *Air Pollution and Cancer*. <https://publications.iarc.fr/Book-And-Report-Series/Iarc-Scientific-Publications/Air-Pollution-And-Cancer-2013>.

- Howe EA, Sinha R, Schlauch D, Quackenbush J. 2011. RNA-Seq analysis in MeV. *Bioinformatics*. 27(22):3209–3210. doi:[10.1093/bioinformatics/btr490](https://doi.org/10.1093/bioinformatics/btr490).
- IARC Working Group on the Evaluation of Carcinogenic Risk to. 2010. Some non-heterocyclic polycyclic aromatic hydrocarbons and some related exposures. International Agency for Research on Cancer.
- Kimlin L, Kassis J, Virador V. 2013. 3D in vitro tissue models and their potential for drug screening. *Expert Opinion on Drug Discovery*. 8(12):1455–1466. doi:[10.1517/17460441.2013.852181](https://doi.org/10.1517/17460441.2013.852181).
- Kirkham PA, Barnes PJ. 2013. Oxidative stress in COPD. *CHEST*. 144(1):266–273. doi:[10.1378/chest.12-2664](https://doi.org/10.1378/chest.12-2664).
- McGuinness AJA, Sapey E. 2017. Oxidative stress in COPD: Sources, markers, and potential mechanisms. *J Clin Med*. 6(2). doi:[10.3390/jcm6020021](https://doi.org/10.3390/jcm6020021). [accessed 2020 May 17]. <https://www.ncbi.nlm.nih.gov/pmc/articles/PMC5332925/>.
- Moorthy B, Chu C, Carlin DJ. 2015. Polycyclic aromatic hydrocarbons: from metabolism to lung cancer. *Toxicol Sci*. 145(1):5–15. doi:[10.1093/toxsci/kfv040](https://doi.org/10.1093/toxsci/kfv040).
- Nebert DW, Roe AL, Dieter MZ, Solis WA, Yang Y, Dalton TP. 2000. Role of the aromatic hydrocarbon receptor and [Ah] gene battery in the oxidative stress response, cell cycle control, and apoptosis. *Biochemical Pharmacology*. 59(1):65–85. doi:[10.1016/S0006-2952\(99\)00310-X](https://doi.org/10.1016/S0006-2952(99)00310-X).
- Rahman I. 2005. The role of oxidative stress in the pathogenesis of COPD: implications for therapy. *Treat Respir Med*. 4(3):175–200. doi:[10.2165/00151829-200504030-00003](https://doi.org/10.2165/00151829-200504030-00003).
- Rao R. 2008. Oxidative stress-induced disruption of epithelial and endothelial tight junctions. *Front Biosci*. 13:7210–7226.
- Schamberger AC, Mise N, Jia J, Genoyer E, Yildirim AÖ, Meiners S, Eickelberg O. 2013. Cigarette smoke-induced disruption of bronchial epithelial tight junctions is prevented by transforming growth factor- β . *Am J Respir Cell Mol Biol*. 50(6):1040–1052. doi:[10.1165/rcmb.2013-0090OC](https://doi.org/10.1165/rcmb.2013-0090OC).
- Shi Q, Godschalk RWL, van Schooten FJ. 2017. Inflammation and the chemical carcinogen benzo[a]pyrene: Partners in crime. *Mutation Research/Reviews in Mutation Research*. 774:12–24. doi:[10.1016/j.mrrev.2017.08.003](https://doi.org/10.1016/j.mrrev.2017.08.003).
- Siddens LK, Bunde KL, Harper TA, McQuistan TJ, Löhr CV, Bramer LM, Katrina MW, Tilton SC, Krueger SK, Williams DE, et al. 2015. Cytochrome P450 1b1 in polycyclic aromatic hydrocarbon (PAH)-induced skin carcinogenesis: tumorigenicity of individual PAHs and coal-tar extract, DNA adduction and expression of select genes in the CYP1b1 knockout mouse. *Toxicol Appl Pharmacol*. 287(2):149–160. doi:[10.1016/j.taap.2015.05.019](https://doi.org/10.1016/j.taap.2015.05.019).
- Siddens LK, Larkin A, Krueger SK, Bradfield CA, Waters KM, Tilton SC, Pereira CB, Löhr CV, Arlt VM, Phillips DH, et al. 2012. Polycyclic aromatic hydrocarbons as skin carcinogens: Comparison of benzo[a]pyrene, dibenzo[def,p]chrysene and three environmental mixtures in the FVB/N mouse. *Toxicol Appl Pharmacol*. 264(3):377–386. doi:[10.1016/j.taap.2012.08.014](https://doi.org/10.1016/j.taap.2012.08.014).
- Stewart CE, Torr EE, Mohd Jamili NH, Bosquillon C, Sayers I. 2012. Evaluation of differentiated human bronchial epithelial cell culture systems for asthma research. *Journal of Allergy*. doi:<https://doi.org/10.1155/2012/943982>.
- Tilton SC, Siddens LK, Krueger SK, Larkin AJ, Löhr CV, Williams DE, Baird WM, Waters KM. 2015. Mechanism-based classification of PAH mixtures to predict carcinogenic potential. *Toxicol Sci*. 146(1):135–145. doi:[10.1093/toxsci/kfv080](https://doi.org/10.1093/toxsci/kfv080).

- Wang C-D, Chen N, Huang L, Wang J-R, Chen Z-Y, Jiang Y-M, He Y-Z, Ji Y-L. 2015. Impact of CYP1A1 polymorphisms on susceptibility to chronic obstructive pulmonary disease: a meta-analysis. *Biomed Res Int*. 2015. doi:[10.1155/2015/942958](https://doi.org/10.1155/2015/942958).
- Wilk A, Rski PW, Lassak A, Vashistha H, LIRETTE D, Tate D, Zea AH, Koochekpour S, Rodriguez P, Meggs LG, et al. 2013. Polycyclic aromatic hydrocarbons—induced ROS accumulation enhances mutagenic potential of T-antigen from human polyomavirus JC. *J Cell Physiol*. 228(11):2127–2138. doi:[10.1002/jcp.24375](https://doi.org/10.1002/jcp.24375).
- Wittekindt OH. 2017. Tight junctions in pulmonary epithelia during lung inflammation. *Pflugers Arch*. 469(1):135–147. doi:[10.1007/s00424-016-1917-3](https://doi.org/10.1007/s00424-016-1917-3).
- Yang L, Allen BC, Thomas RS. 2007. BMDExpress: a software tool for the benchmark dose analyses of genomic data. *BMC Genomics*. 8(1):387. doi:[10.1186/1471-2164-8-387](https://doi.org/10.1186/1471-2164-8-387).
- Yang L, Wang W-C, Lung S-CC, Sun Z, Chen C, Chen J-K, Zou Q, Lin Y-H, Lin C-H. 2017. Polycyclic aromatic hydrocarbons are associated with increased risk of chronic obstructive pulmonary disease during haze events in China. *Science of The Total Environment*. 574:1649–1658. doi:[10.1016/j.scitotenv.2016.08.211](https://doi.org/10.1016/j.scitotenv.2016.08.211).